SUPPORTING INFORMATION

Lead minerals found in drinking water distribution systems increase chlorine dioxide decay to a single inorganic by-product

Margaret M. Reuter, Christian M. Lastoskie*

Department of Civil and Environmental Engineering, 1351 Beal Avenue, University of Michigan, Ann Arbor, MI 48109, USA

*Corresponding author: Phone: (734) 647-7940. Email: cmlasto@umich.edu

12 pages, 7 figures. 2 tables, calculation of rate models, calculation of electron supply

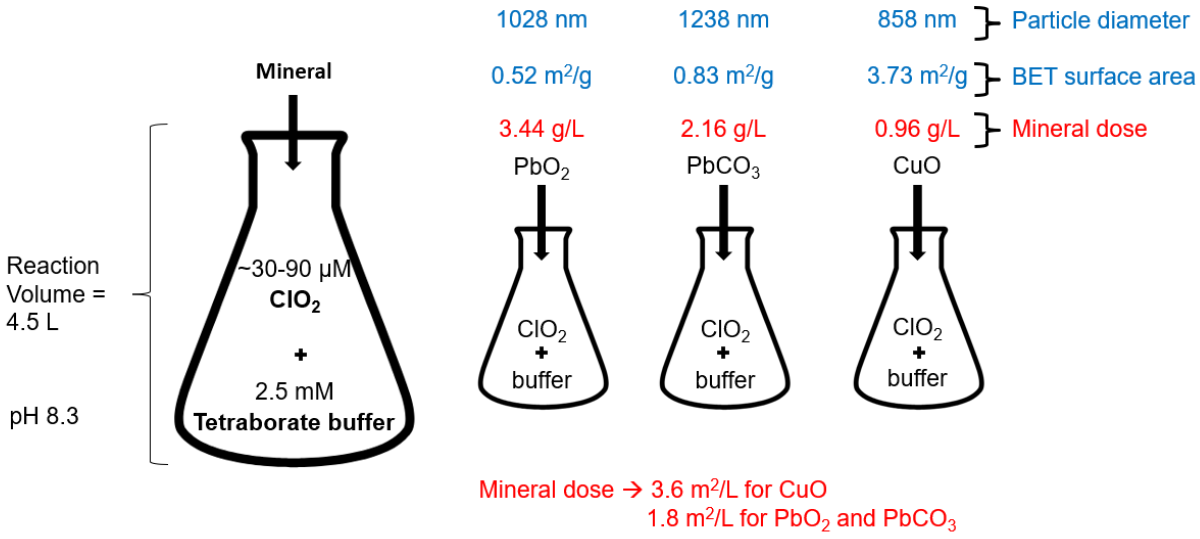

Figure S1. Graphic illustration of batch reactions and experimental parameters.

Table S1. Characteristics and dose of scale minerals used in batch reactions.

Compound	**BET surface area ($m^2 g^{-1}$)**	**Particle diameter (nm)**	**Reaction surface area ($m^2 L^{-1}$)**	**Mass dose ($g L^{-1}$)**
PbO_2	0.52	1028	1.8	3.4
$PbCO_3$	0.83	1238	1.8	2.2
CuO	3.73	858	3.6	0.96

Notes on the chlorine balance

The initial starting concentration of ClO_2 in the batch reactor was measured and adjusted to a target of 50 μM. However, the chlorine balances in the batch reactors were affected by the presence of chlorite at the initial conditions, ranging in concentration from 0 to 9 μM. Chloride was also sampled for during the batch reactions, but its concentrations were found to be insignificant. While the initial total chlorine concentration in the system is thus not uniform, the chlorine balance is nevertheless closed.

The presence of the chlorite detected at the outset of some of the batch experiments could be due to chlorite formation as a decay product in the ClO_2 stock solution. While a scrubber solution was used to remove as much chlorite as possible during the production of the ClO_2 stock solution, some chlorite residual may nonetheless still be left in solution. Chlorite can also form in the batch reactor prior to mineral addition while the ClO_2 concentration is being calibrated, although without a mineral catalyst, ClO_2 decay is relatively slow, as shown for the blank sample in Figure 2. Variability in the chlorine balance could also be due to inadequate sparging of ClO_2 before ion chromatography samples were taken. Sparging with nitrogen gas was performed for ten minutes, but trace amounts of ClO_2 in the samples could form chlorite while awaiting analysis. Other sources of experimental error that were considered include ClO_2 loss during filtration and chlorite formation while samples were queued for sparging.

Rate models

Six different rate models were considered for the analysis of chlorine dioxide decay: first-order, second-order, mixed-order (simultaneous first and second order reactions), two-phase (two simultaneous first-order reactions), pseudo-first order adsorption, and pseudo-second order adsorption. Rate constants are reported in Table S2 for second order and pseudo-second order models. Despite matching the proposed reaction mechanism, first-order models were significantly worse at fitting the batch reactor data than any of the other models. The two-phase model yields a better-quality fit to the decay rate data (as measured by the coefficient of determination, R^2) than either the second-order or mixed-order model.

The mixed-order model was used in previous studies to interpret chlorine dioxide decomposition in basic solutions.[1] The rate constants essentially followed a second order decay, as the first order rate constant was nearly equal to zero. A second order model was found to best fit the rate data measured at pH 8.3. At pH values above and below the zero-point pH, there is an initial phase of lead oxide surface reacting with chlorine dioxide. As the experiment progresses the lead surface becomes populated with charged ions, positive or negative depending on whether the experiment was conducted above or below the point of zero charge. The kinetic rates slow as the surface becomes blocked for chlorine dioxide adsorption. Perhaps these surface interactions are incorporated into the two-phase model, where the phases represent (1) the first-order reaction of chlorine dioxide on the lead surface, and (2) the reduction of surface sites for the reaction to take place.

The pseudo-first order (Equation 5) and pseudo-second order (Equation 6) models incorporate adsorption kinetics and sorbent capacity into the chlorine dioxide decay rate constants.[2,3] These models have been used in the kinetic analysis of free chlorine adsorption on

lead (IV) oxide at different pH values. For the chlorine dioxide decay rate analysis, the concentration of adsorbed chlorine dioxide (q_e in µg of ClO_2/g) was taken to be the difference between the initial aqueous chlorine dioxide concentration and the aqueous ClO_2 concentration at time t (q_t in µg of ClO_2/g). Rate constants k_1 (min^{-1}) and k_2 (g/µg of $ClO_2 \cdot min$) were calculated for pseudo-first and pseudo-second order models respectively.[2,3]

$$log(q_e - q_t) = \log q_e - \frac{k_1}{2.303} t \quad (5)$$

$$\frac{t}{q_t} = \frac{1}{k_2 q_e^2} + \frac{1}{q_e} t \quad (6)$$

Chlorine dioxide adsorption follows pseudo-second order adsorption based on the R^2 values (Table S2). These results suggest that hydroxide ions are in excess and then the reaction is dependent on chlorine dioxide concentration. Previously published work demonstrated copper, nickel, and iron enhancement of chlorine dioxide decay followed a second-order dependence on chlorine dioxide.[4]

A secondary consideration is the phase of the lead mineral itself. The oxidation reduction potential for chlorine dioxide is high,[5] and for pH levels relevant to drinking water, lead (IV) oxide is favored to form.[6,7] At lower pH, the mineral surface could be changing composition to lead carbonate, which has a slower reaction rate with chlorine dioxide than lead oxide. The phase shift from lead (IV) oxide to lead (II) carbonate could also point to why a second order model is statistically unfavorable at pH less than 7. In this case the first phase rate constant corresponds to the presence of lead oxide and is more rapid than the second phase rate constant, corresponding to a new surface of lead carbonate.

Table S2. Rate constants and R^2 values for two different exponential decay models fit to chlorine dioxide decay in the presence of lead oxide at varying pH values.

pH	**Second order decay**		**Pseudo-second order adsorption**	
	Rate (M^{-1} s^{-1})	**R^2**	**Rate (M^{-1} s^{-1})**	**R^2**
5.9	14±3	0.58	267.6±0.7	0.994
7.4	58±8	0.92	166.3±0.4	0.988
8.3	200.±20.	0.98	290.4±0.1	0.999
9.7	26±4	0.87	156.0±0.9	0.968
10.4	20.±4	0.76	87.8±0.7	0.965

Electron supply

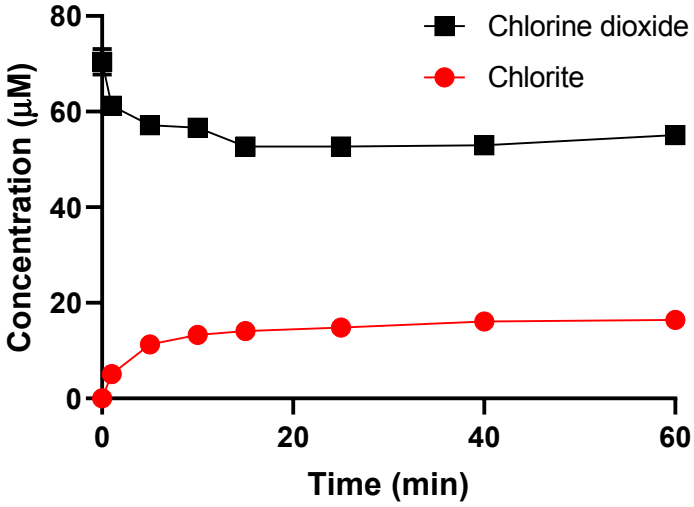

Figure S2. Chlorine dioxide decay and chlorite formation in an unbuffered batch reaction with PbO_2. Each data point represents the mean and standard deviation of duplicate experiments. If error bars were shorter than the symbol, they were removed.

The two unbuffered batch reactions were done in Milli-Q water, a starting chlorine dioxide concentration of about 70 µM, and the same PbO_2 dose as the buffered reactions. They were performed to confirm the oxidation of water via pH measurements.

Chlorine dioxide oxidizes water (eq 1).

$$ClO_2 + \frac{1}{2}H_2O = \frac{1}{4}O_2 + ClO_2^- + H^+ \quad (1)$$

In an unbuffered system this corresponds to a drop in pH (eq 2 and 3):

$$-\Delta ClO_2 = \Delta H^+ \quad (2)$$

$$pH = -\log [H^+] \quad (3)$$

The change in chlorine dioxide concentration in both replicates of the unbuffered batch reaction had a theoretical pH of 4.76 and 4.79, and measured pH of 5.1 and 4.8 respectively.

Figure S3. Lead carbonate batch reaction over the course of one hour. Image 1 was taken immediately upon the addition of lead carbonate. Images 2 and 3 are taken after late batch reaction samples.

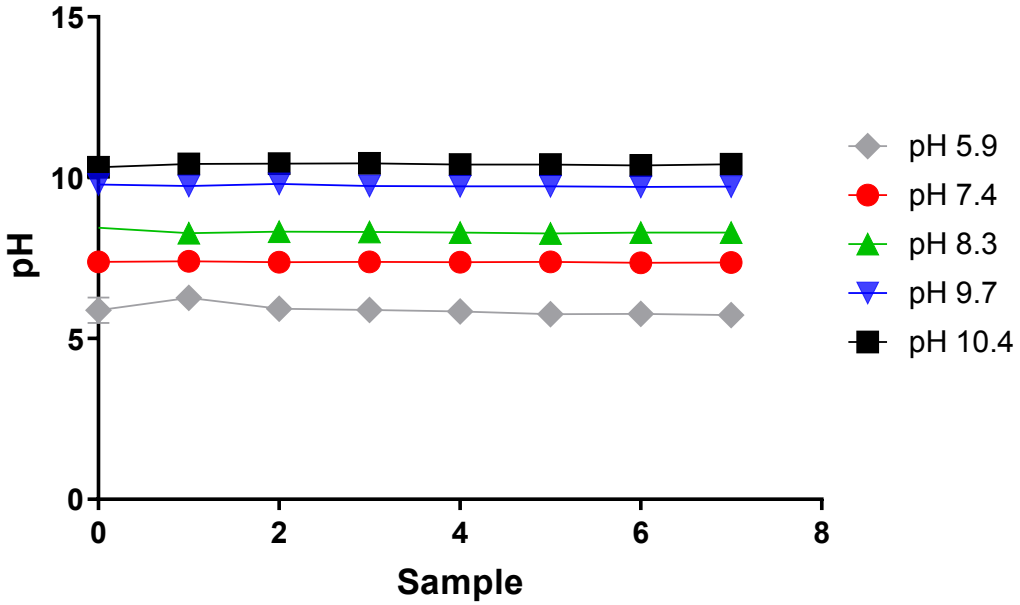

Figure S4. Variation in pH during pH batch experiments corresponding to Figure 3. At pH 5.9 and pH 7.4 the variation was 0.5. Above pH 8.3 there was less than 0.03 change in pH.

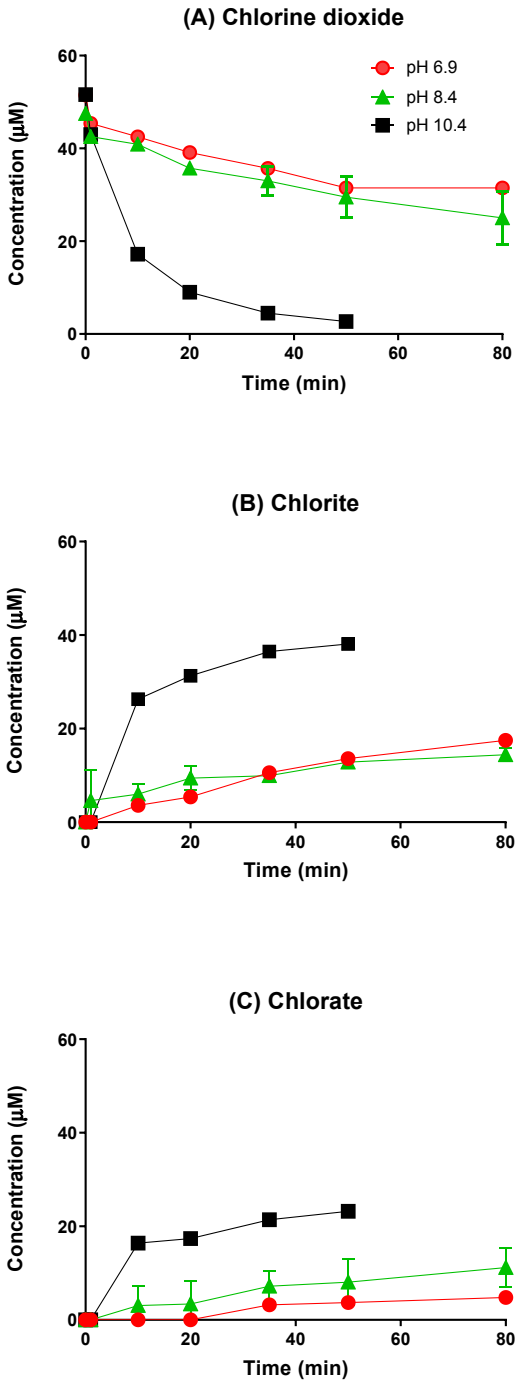

Figure S5. (A) Chlorine dioxide decay, (B) chlorite formation, and (C) chlorate formation in batch reactions containing chlorine dioxide and cupric oxide at three different pH values. Each data point represents the mean and standard deviation of duplicate experiments. If error bars were shorter than the symbol, they were removed.

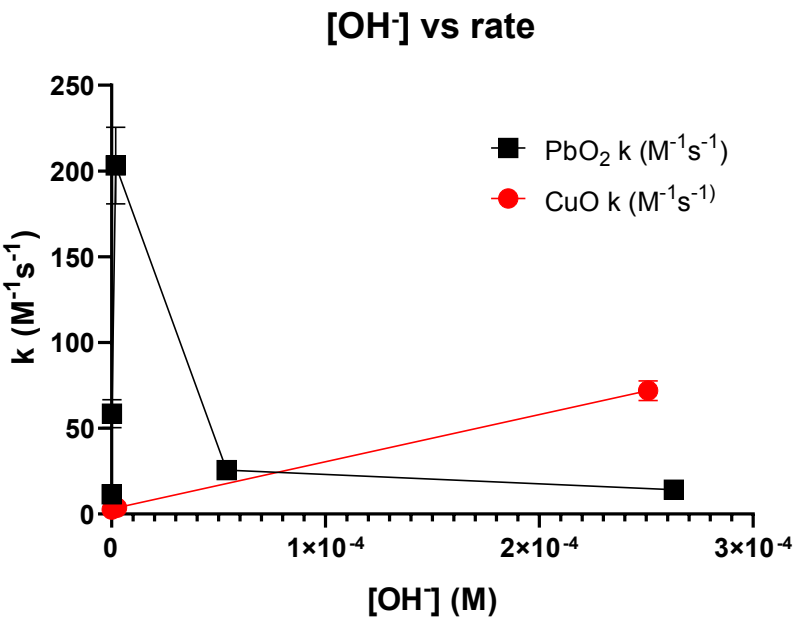

Figure S6. Relationship between measured second-order rate constants and hydroxide concentration. Batch experiments with CuO showed a linear dependence on [OH^-], while PbO_2 showed no dependence and a maximal rate at pOH 5.7 (pH 8.3).

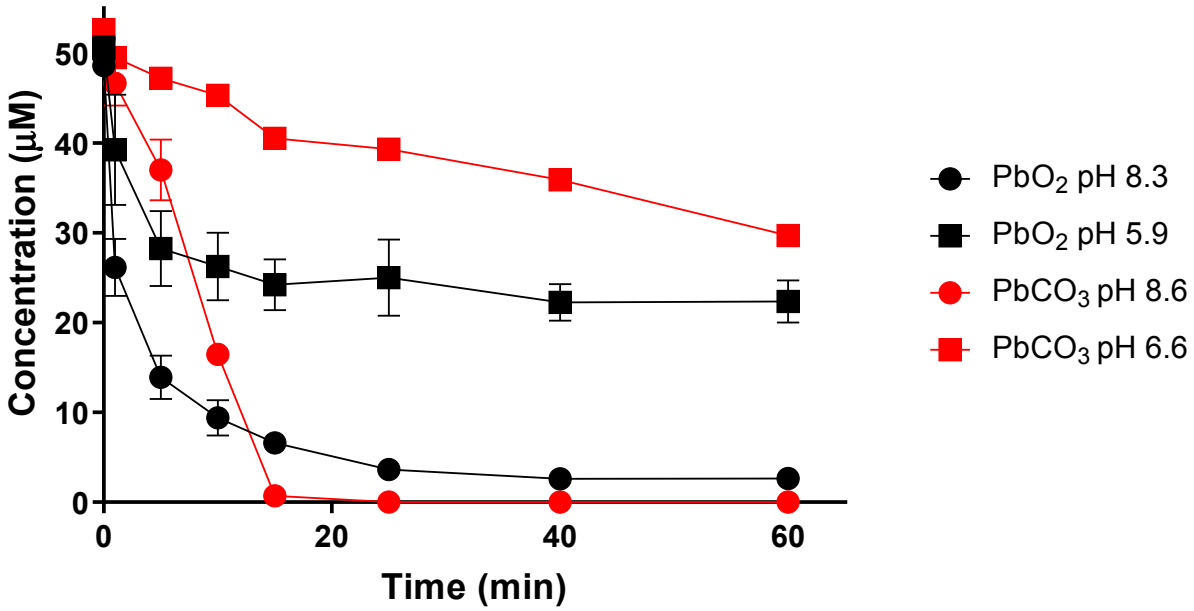

Figure S7. Chlorine dioxide decay in batch reactions at different pH and in the presence of lead carbonate (red) or lead oxide (black). Each data point represents the mean and standard deviation of duplicate experiments. If error bars were shorter than the symbol, they were removed.

References

1 I. N. Odeh, J. S. Francisco and D. W. Margerum, New pathways for chlorine dioxide decomposition in basic solution, *Inorg. Chem.*, 2002, **41**, 6500–6506.

2 S. Ho, Y. and G. McKay, Pseudo-second order model for sorption processes, *Process Biochem.*, 1999, **34**, 451–465.

3 Y. Zhang and Y.-P. Lin, Adsorption of Free Chlorine on Tetravalent Lead Corrosion Product (PbO2), *Environ. Eng. Sci.*, 2012, **29**, 52–58.

4 C. Liu, U. Von Gunten and J.-P. P. Croue, Enhanced chlorine dioxide decay in the presence of metal oxides: Relevance to drinking water distribution systems, *Environ. Sci. Technol.*, 2013, **47**, 8365–8372.

5 C. James, R. Copeland and D. Lytle, Relationships between oxidation-reduction potential, oxidant, and pH in drinking water, *Proc. AWWA Water Qual. Technol. Conf.*, 2004, 1–13.

6 D. A. Lytle and M. R. Schock, Formation of Pb(IV) oxides in chlorinated water, *J. Am. Water Work. Assoc.*, 2005, **97**, 102–114.

7 D. A. Lytle, M. R. Schock and K. Scheckel, The inhibition of Pb(IV) oxide formation in chlorinated water by orthophosphate, *Environ. Sci. Technol.*, 2009, **43**, 6624–6631.